Rotational energy transfer in hydrogen halide molecules at supersonic beam velocities

Alexander F. Turfa[a] and R. A. Marcus

Arthur Amos Noyes Laboratory [b] *of Chemical Physics, California Institute of Technology, Pasadena, California 91125*

(Received 19 October 1978)

Rotational energy transfer cross sections are calculated for HCl–HCl and HCl–HF collisions using classical trajectories. The exponential model for the rotational results is compared with transitions $j \to j'$ in collisions of a supersonic HCl molecular beam with a thermal beam. Reasonable agreement with the functional form of that model is obtained. Using a simple intermolecular potential without adjustable parameters, in which the only anisotropic terms are of the dipolar and dispersion type (i.e., long range), agreement is obtained with the experimental constant for HCl–HCl in the exponential. Calculations are also given for HCl–HI and HCl–HBr collisions. Microscopic reversibility for the averaged cross sections is discussed in connection with the exponential model. The trajectory results show that some modification is needed in the exponential formula, to account for microscopic reversibility in these rotor–rotor collisions.

I. INTRODUCTION

Many theoretical calculations have employed classical mechanics to describe molecular translational–rotational energy transfer for collisions between atoms with linear molecules, treated as rigid rotors.[1] In the present paper, classical trajectories for collisions between two linear rigid rotors[2] are used to compute the cross sections $\sigma(j,j')$, for an HCl molecule in a supersonic primary beam to undergo the collisional transition, $j \to j'$, when this fast primary beam is crossed with a thermal beam of a hydrogen halide. Throughout, the unprimed quantity refers to the value of a dynamical variable before a collision, while the primed quantity denotes its postcollisional value. The calculated values of $\sigma(j,j')$ for several HCl–hydrogen halide collision systems are compared with the exponential model proposed by Polanyi *et al.*,[3]

$$\sigma(j,j') = C_1(2j'+1)\exp(-C\,|E_j - E_{j'}|)\,, \tag{1}$$

where C_1 and C can both depend on the total energy and are characteristic of a particular collision pair. (The collision partner will be termed the "perturber".) Under the conditions of the experiment[3(a)] the initial relative kinetic energy of the molecules was about 30 kcal/mole, and exceeded the rotational energies by factors of the order of 50.

By spectroscopically monitoring the primary HCl beam before and after it crossed a thermal beam, Ding and Polanyi[3(a)] directly measured $\Delta N(j)$, the change in the population of the jth rotational state of the HCl molecules. By plotting the measured $\Delta N(j)$ vs j and by comparing with the plot predicted by the exponential model, they inferred the value of C in Eq. (1). This value is compared with that calculated in the present work. Previously, classical trajectory calculations of $\sigma(j,j')$ have been performed for the HCl–Ar[3(c),3(e),4] system and compared with the exponential model.[3(a)]

Values of $\sigma(j,j')$ for the HCl–hydrogen halide systems are computed in the present paper for three different initial states, $j=0$, 4, and 8, together with total inelastic cross sections $\sigma(j)$:

$$\sigma(j) = \sum_{j' \neq j} \sigma(j,j')\,. \tag{2}$$

In the case of atom–rigid linear molecular collisions the equation of microscopic reversibility is

$$k^2(2j+1)\,\sigma(j,j') = k'^2(2j'+1)\,\sigma(j',j)\,, \tag{3}$$

where k denotes the translational wave number. In the experiments of Ref. 3(a), the initial translational energies for the molecules in the beam of about 30 kcal/mole in each system are much greater than the rotational energy of even the eighth level of either molecule, the approximation that the ratio of final to initial velocities $v'/v(=k'/k) \approx 1$ is appropriate here. Equation (1) then satisfies the microscopic reversibility relation (3). We shall also explore the extent to which (3) and hence Eq. (1) satisfy microscopic reversibility for collisions between two rigid rotors.

II. CALCULATIONS

The total angular momentum $\hat{J}$ representation, with $\hat{J}$ placed along the z axis, was used to treat the dynamics.[2] Using a subscript p to denote the angular momentum of the second molecule, the variables in the coupled action-angle representation of Ref. 2 are the magnitudes of $\hat{J}$, of the rotational angular momenta of the two rotors, $\hat{j}$ and $\hat{j}_p$, of the orbital angular momentum $\hat{l}$, and of the resultant $\hat{h}$ ($\mathrm{h} = \mathrm{j}_p + 1$). There are also the angles conjugate to $\hat{j}$, $\hat{j}_p$, $\hat{l}$ and $\hat{h}$ (q_j, q_{j_p}, q_l, q_h), the intermolecular separation distance R, and its conjugate momentum p_R. These variables are described in Figs. 1–3 of Ref. 2(b).

In determining transition probabilities via the Monte Carlo method, each trajectory was started at a separation distance R_0, chosen so that at R_0 the intermolecular potential energy is less than 1% of thermal energy (k_BT) at 300 °K.[2(b)] Hamilton's equations with rigid rotor constraint [Appendix A of Ref. 2(a)] were integrated numerically for a specified interaction potential

[a] Present address: Department of Chemistry, The University of Manchester, Manchester, M13 9PL, England.

[b] Contribution No. 5899.

 0021-9606/79/063035-06$01.00

function while the two molecules collide. When the separation was again $R \geq R_0$, the integration was stopped. Transition probabilities were calculated quasiclassically by noting which interval $(j' - \frac{1}{2}, j' + \frac{1}{2})$ the postcollision value of the quantum number j' was in, and counting such trajectories towards the transition probability for $j \to j'$. The quantum numbers j are related to the corresponding angular momenta $\hat{j}$ semiclassically by Eq. (4) in units of $\hbar = 1$,[2]

$$\hat{j} = j + \tfrac{1}{2} . \tag{4}$$

Instead of q's, time-independent angle variables $\bar{w}$ (obtained by a canonical transformation) were used.[2]

The cross section for a transition $j \to j'$ is given by

$$\sigma(j,j') = \int_0^\infty P(j, j', b)\, 2\pi b\, db , \tag{5}$$

where

$$P(j, j', b) = \int_0^\infty \rho_{j_p} d\hat{j}_p \int_{\hat{j}_p - \hat{l}}^{\hat{j}_p + \hat{l}} d\hat{h}(\hat{h}/2\hat{j}_p \hat{l}) \times \int_{|\hat{h}-\hat{j}|}^{\hat{h}+\hat{j}} d\hat{J}(\hat{J}/2\hat{h}\hat{j}) \int_0^1 \cdots \int_0^1 P(j, j')\, d\bar{w} . \tag{6}$$

Here, $d\bar{w}$ denotes $d\bar{w}_h d\bar{w}_l d\bar{w}_{j_p} d\bar{w}_j$; ρ_{j_p} denotes the Boltzmann distribution of perturber rotational states; $P(j,j')$ denotes the probability of the $j \to j'$ collisional transition for a given set of initial conditions, being 1 or 0 accordingly as the trajectory determined by those initial conditions does or does not result with a value of j' within the interval $(j' - \frac{1}{2}, j' + \frac{1}{2})$. The integral in Eqs. (5) and (6) can be evaluated by sampling the eight variables $(b, \hat{j}_p, \hat{h}, \hat{J}, \bar{w}_h, \bar{w}_l, \bar{w}_{j_p}, \bar{w}_j)$, introducing new variables x_i so that all lie in an interval (0, 1) (cf. Appendix A and Ref. 2). The impact parameter b yields the value of the orbital angular momentum $\hat{l}$, being equal to $\hat{l}/p_R$.

Instead of Eq. (6) a semiclassical calculation was used in Ref. 2, wherein the mean probability term $\int_0^1 P(j,j')\, d\bar{w}_j$ is replaced by $|dj'/d\bar{w}_j|^{-1}$, evaluated at a $\bar{w}_j$ (for the given remaining $\bar{w}$'s and momenta) which gives rise to the desired final j'. When more than one $\bar{w}_j$ gave the desired final j', this probability was a sum over such derivatives.

The values of the total inelastic cross section of $\sigma(j)$ are computed from

$$\sigma(j) = \int_0^\infty [1 - P(j,j,b)] 2\pi b\, db . \tag{7}$$

The intermolecular potential used in the present calculations consists of a spherically symmetric repulsive core V_{rep}, as in the first term of Eq. (2.1) of Ref. 2(b),

TABLE I. Total rotational inelastic cross sections (Å^2) $\sigma(j)$ for hydrogen halide systems.

System	$\sigma(0)$	$\sigma(4)$	$\sigma(8)$
HCl–HCl	92 ± 2	95 ± 2	60 ± 2
HCl–HF	109 ± 2	127 ± 3	109 ± 3

TABLE II. Rotational cross sections (Å^2) for HCl–HCl.

j' \ j	0	4	8
0		1.2 ± 0.2	
1	47.8 ± 2.0	4.4 ± 0.4	
2	19.8 ± 0.8	9.6 ± 0.6	
3	12.3 ± 0.6	35.5 ± 1.7	0.49 ± 0.13
4	7.2 ± 0.4		2.6 ± 0.3
5	4.2 ± 0.3	32.6 ± 2.0	4.8 ± 0.4
6	0.98 ± 0.15	7.4 ± 0.5	8.2 ± 0.5
7		2.9 ± 0.3	23.6 ± 1.3
8		1.5 ± 0.2	
9		0.24 ± 0.08	16.1 ± 1.0
10			3.5 ± 0.3
11			0.87 ± 0.15
12			0.23 ± 0.07

a dipole–dipole term V_{dd}, and dispersion terms V_{disp}, as in Eqs. (2.7) and (2.4) of Ref. 2(b). The values of the molecular parameters used in this work in the notation appearing in those equations, namely, of ϵ/k, σ, μ, B, $\alpha^{\parallel}$, $\alpha^{\perp}$, are 344.7 °K,[5] 3.339 Å,[5] 1.08 D,[6] 10.5909 cm^{-1},[7] 2.807 Å^3,[8] and 2.497 Å^3,[8] respectively, for HCl. The corresponding values used for HF are 330,[5] 3.148,[5] 1.82,[6] 20.939,[7] 0.96,[9] and 0.72,[9] respectively. Those for HBr and HI are given in Appendix B.

III. RESULTS

Tables I–III summarized the present results for HCl–HCl and HCl–HF: The total inelastic cross sections $\sigma(j)$ are given in Table I for $j = 0$, 4, and 8 and the individual $\sigma(j,j')$'s are given in Tables II and III. The (±) uncertainties noted here are those associated with a 68% confidence limit in Monte Carlo[2,10] calculations. The sampling of the impact parameters was performed in such a way as to yield minimum error in the total inelastic cross section $\sigma(j)$, as in Appendix A, rather than for any one $\sigma(j,j')$. An estimate of the error for $\sigma(j)$ is seen from Table II to be about 2–3%. Tables II

TABLE III. Rotational cross sections (Å^2) $\sigma(j,j')$ for HCl–HF.

j' \ j	0	4	8
0		1.7 ± 0.3	
1	52.1 ± 2.1	6.0 ± 0.5	
2	20.3 ± 1.0	13.2 ± 0.8	1.0 ± 0.2
3	12.7 ± 0.7	50.5 ± 2.4	3.2 ± 0.3
4	9.3 ± 0.6		4.6 ± 0.4
5	7.3 ± 0.5	39.4 ± 2.3	7.8 ± 0.6
6	4.6 ± 0.4	9.2 ± 0.6	15.7 ± 0.9
7	2.3 ± 0.3	3.6 ± 0.4	45.1 ± 2.2
8	0.83 ± 0.18	2.0 ± 0.3	
9		1.2 ± 0.2	24.1 ± 1.5
10		0.44 ± 0.13	4.6 ± 0.5
11			1.5 ± 0.2
12			0.9 ± 0.19

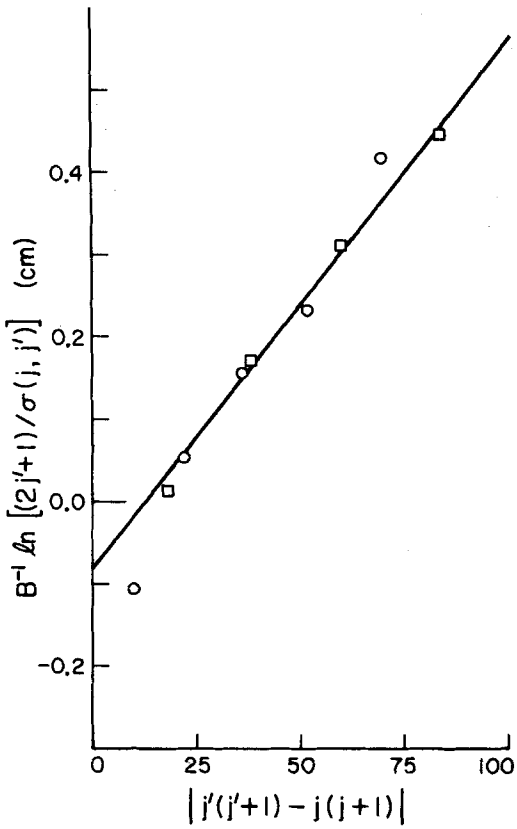

FIG. 1. Plot of $\ln[2j'+1)/\sigma(j,j')]/B$ vs $|j'(j'+1)-j(j+1)|$ for excitation transitions ($j'>j$) for the HCl–HCl system. The circles refer to $j=4$ and the squares to $j=8$.

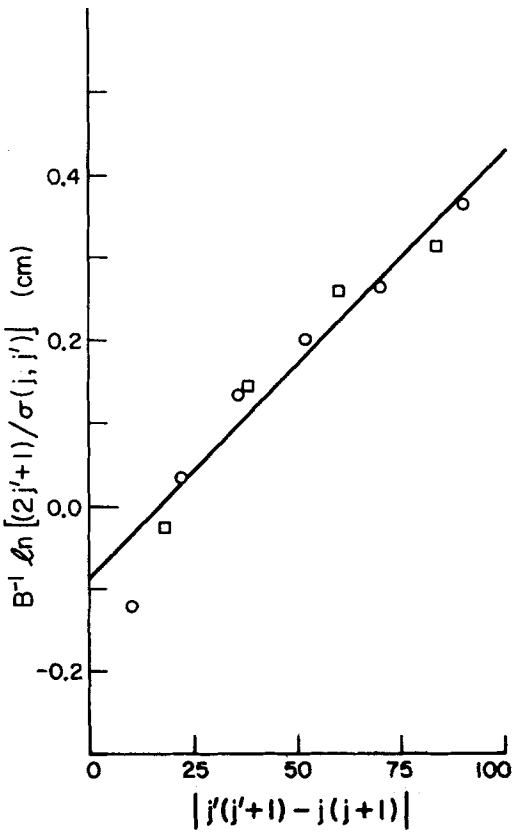

FIG. 3. Plot of $\ln[(2j'+1)/\sigma(j,j')]/B$ vs $|j'(j'+1)-j(j+1)|$ for excitation transitions ($j'>j$) for the HCl–HF system. The circles refer to $j=4$ and the squares to $j=8$.

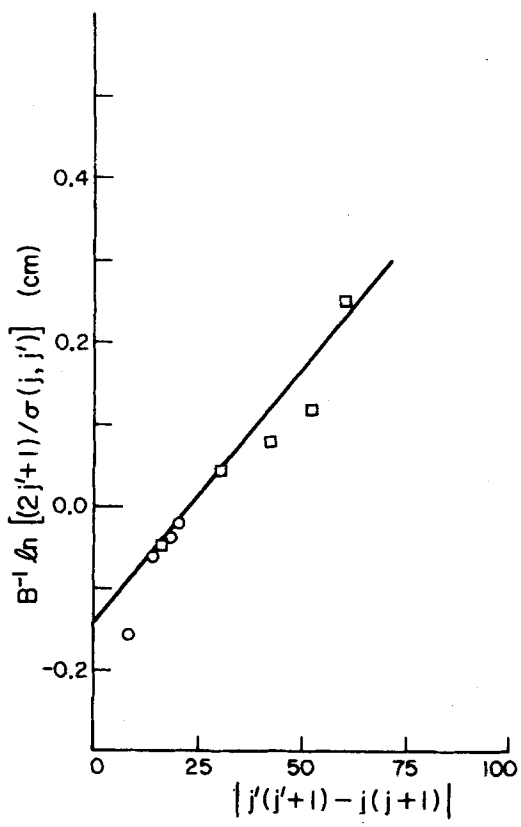

FIG. 2. Legend same as Fig. 1, but for de-excitation transitions ($j'<j$).

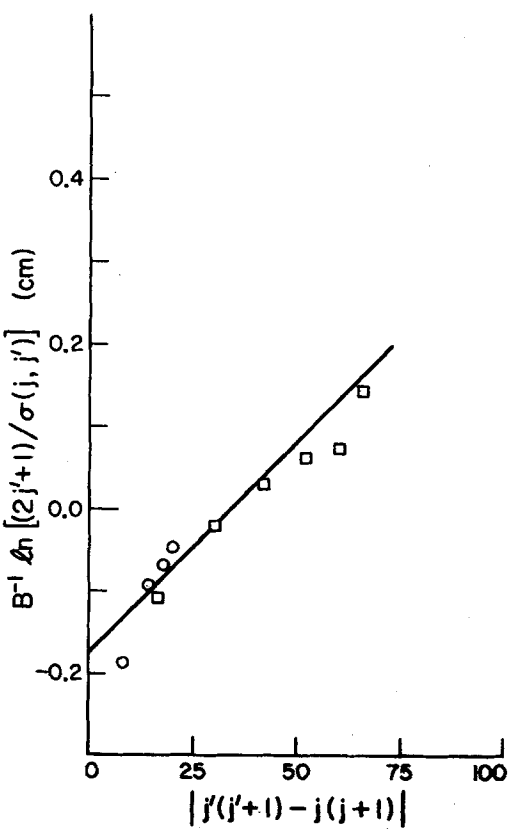

FIG. 4. Legend same as Fig. 3, but for de-excitation transitions.

and III contain the $\sigma(j,j')$'s for which the standard error is less than about 35%.

The constant C in Eq. (1) is obtained as the slope of a $\ln[(2j'+1)/\sigma(j,j')]/B$ vs $|j'(j'+1)-j(j+1)|$ plot, where B is the rotational constant of HCl. The results are plotted in Figs. 1–4. The $j=4$ and $j=8$ points are seen to lie on the same line. The slopes for the excitation transitions ($j'>j$) for the $j=4$ and 8 systems in Figs. 1 and 3 yield C values of 0.006 cm and 0.005 cm for the HCl–HCl and HCl–HF systems, respectively. The slopes of the de-excitation plots (Figs. 2, 4) are the same as those in Figs. 1 and 3, within the errors. There may be some tendency for departure from linearity at low energy transfers, a point to which we return later (cf. an analogous result for HCl–Ar).[4]

The excitation points for $j=0$ are not shown in Figs. 1 and 3. They lie near the lines drawn, but tend to be crowded into a curved portion of the plots at low $|j'(j'+1)-j(j+1)|$.

Deviations from the atom–rigid rotor microscopic reversibility relation (3) show up in Figs. 1–4, in that the intercepts of the excitation plots (Figs. 1, 3) are not the same as those of the de-excitation plots (Figs. 2, 4). A sharper test of (3) and hence of this "microscopic reversibility" aspect of (1) is given in Table IV, where use is made of the fact that $k'\cong k$ to a high accuracy. Tests of a microscopic reversibility relation described in the next section are also given, and serve as tests of the accuracy of the trajectory data.

IV. DISCUSSION

The trajectory-calculated values of C for the HCl–HCl and HCl–HF systems were 0.006 cm and 0.005 cm, respectively, as already noted. The former agrees well with the experimentally determined value of C of 0.006 cm.[3(a)] In the cases of HCl–HBr and HCl–HI (Appendix B), however, the calculated C values were greater than those inferred from measurements, considerably so in the HCl–HI case. Thereby, the calculated distribution of final rotational states of HCl in those collisions is narrower than the experimental one deduced from the value of C. In collisions of HCl–HI, the calculated total inelastic cross sections were substantially smaller than that for HCl–HCl and HCl–HF (Appendix B), so short range anisotropic repulsive potentials should be included in any potential used. The anisotropy of the potential used in the present calculations contained only long range (dispersive and dipolar) terms.

It is seen from the first two columns of numbers in Table IV that the microscopic reversibility relation (3), strictly valid for atom–rigid rotor (linear molecule) collisions, is not obeyed by the appropriate ratios of cross sections. The discrepancy is greater for the $\sigma(4,8)/\sigma(8,4)$ ratio than for the $\sigma(0,4)/\sigma(4,0)$ one. Because of the small fraction of the total number of trajectories contributing to these highly inelastic transitions, there is a standard error of about 20% associated with these ratios in Table IV, which are nevertheless sufficiently precisely determined to provide a reliable test for adherence to Relation (3). Thus, since (1) satisfies (3) it does not describe this aspect of microscopic reversibility accurately for rotor–rotor collisions, although it does represent the logarithmic plots in Figs. 1–4 reasonably well. We explore this breakdown next.

TABLE IV. Test for "microscopic reversibility."[a]

System	$\frac{\sigma(0,4)}{9\sigma(4,0)}$	$\frac{9\sigma(4,8)}{17\sigma(8,4)}$	$\frac{\langle f\rangle\sigma(0,4)}{9\sigma(4,0)}$	$\frac{\langle f\rangle 9\sigma(4,8)}{17\sigma(8,4)}$
HCl–HCl	0.66 ± 0.14	0.30 ± 0.07	1.11 ± 0.30	1.32 ± 0.40
HCl–HF	0.62 ± 0.14	0.23 ± 0.05	0.94 ± 0.27	0.88 ± 0.34

[a]A ratio of unity for the first two columns yields agreement with Eq. (3) and, for the last two columns, with Eq. (12).

For a rigid rotor–rigid rotor system one has instead of Eq. (3),

$$k^2(2j+1)(2j_p+1)\sigma(jj_p, j'j'_p) = k'^2(2j'+1)(2j'_p+1)\sigma(j'j'_p, jj_p)\ . \tag{8}$$

This equation is next multiplied by $(\bar{k}'/k')^2\exp(-E'_{jp}/k_BT)/Q_p$, where $\bar{k}'$ is defined by an atom–rigid rotor energy conservation, setting $\hbar=1$,

$$E_j+k^2/2\mu = E_{j'}+\bar{k}'^2/2\mu\ , \tag{9}$$

and Q_p is the rotational partition function of the pertuber. Upon integration over j_p and j'_p, one obtains

$$k^2(2j+1)\sigma(j,j')\langle(\bar{k}'/k')^2 \times \exp[(E_{jp}-E'_{jp})/k_BT]\rangle = \bar{k}'^2(2j'+1)\sigma(j',j)\ , \tag{10}$$

where $\sigma(j,j')$ is the denominator in the following expression, $\langle f\rangle$ is

$$\langle f\rangle = \int\int f\sigma(jj_p,j'j'_p)\,\rho_{jp}\,dj_p\,dj'_p \times\left(\int\int\sigma(jj_p,j'j'_p)\,\rho_{jp}\,dj_p\,dj'_p\right)^{-1}\ , \tag{11}$$

and ρ_{jp} is $(2j_p+1)\exp(-E_{jp}/k_BT)/Q_p$. Apart from the factor $\langle\ \rangle$, Eq. (10) is identical with the atom–rigid rotor microscopic reversibility relation (3).

Under the conditions of Ref. 3(a), $\bar{k}\cong k'\cong k$ and (10) becomes

$$(2j+1)\sigma(j,j')\times\langle\exp[(E_{jp}-E'_{jp})/kT]\rangle = (2j'+1)\sigma(j',j)\ . \tag{12}$$

To test this equation, the same trajectories used to calculate $\sigma(j,j')$ and $\sigma(j',j)$ were also used to calculate the quantity in brackets. The results are given in the last two columns of Table IV. The microscopic reversibility relation (12), unlike (3), is seen to be satisfied within the estimated errors, as indeed it should be. The percent standard errors associated with the ratios in the last two columns in Table IV are about 30%, slightly larger than those for the ratios in the previous two columns. The errors are small enough to make possible a meaningful test of the relation (12).

If there were resonant rotational transfer, i.e., if $E_j+E_{jp}=E'_j+E'_{jp}$, then $E_{jp}-E'_{jp}$ would be E'_j-E_j and so $\langle\exp(E_{jp}-E'_{jp})/k_BT\rangle$ would exceed unity when $j<j'$.

Therefore, one sees from (12) that the ratios in the first two numerical columns in Table IV should be less than unity, as found. Since $E'_j - E_j$ is much greater for the 4 – 8 transition than for the 0 – 4 one, the deviation from unity should be much larger for the former transfer than the latter, again as found. However, tendency towards resonance is only an approximate one, for if it were an exact one, one could simply replace $\langle f \rangle$ by $\exp(E'_j - E_j)/k_B T$ as a correction factor. This factor is about 14 for the 4 – 8 transition for HCl–HCl, whereas the true $\langle f \rangle$ is only about a factor of 4.

It is seen in Figs. 1–4 that a departure from linearity occurs for the point with the smallest $|E'_j - E_j|$. Because of the nature of the classical calculations a well-known infinity develops in the total elastic cross sections—unless some cutoff in scattering angle is introduced into the classical definition of the cross section. This infinity occurs, thereby, at $j' = j$ and the effects of this singularity do not immediately disappear as j' moves away from j. Thus, there is at least the possibility that at small $|E'_j - E_j|$ the trajectory-calculated rotational inelastic cross section may be too high {i.e., $\ln[(2j'+1)/\sigma(j,j')]$ too low}, and so could account for this particular deviation in Figs. 1–4. An alternative possibility is that Eq. (1) breaks down at low $|E'_j - E_j|$. A comparison of (1) with quantum results would therefore be especially useful.

In summary, the simple expression (1) is reasonably well obeyed for the $j = 4$ and $j = 8$ systems studied, apart from the microscopic reversibility aspect embodied in (12) and illustrated in Table IV. Classical mechanics plus the present potential which has no adjustable parameters yields reasonable agreement with the experimentally derived[3(a)] C value for the inelastic rotational transitions for HCl–HCl. It will be useful to compare the absolute values of the individual cross sections when they become available. The intermolecular potential used here contains in its anisotropic part the sum of dipole–dipole and dispersion forces. For systems like HCl–HI, it appears that additional, short range, anisotropic terms, probably repulsive, will be needed. This result is not surprising in view of the relatively small calculated cross section (see Appendix B). Total inelastic experimental cross sections would be useful in this respect.

The calculated cross sections obey the principle of microscopic reversibility (12). Some tendency towards resonant energy transfer prevents the atom–diatomic molecule microscopic reversibility relation (3) from being obeyed when the highly inelastic $j \rightleftharpoons j'$ transitions (0 ⇌ 4) and (4 ⇌ 8) are considered.

ACKNOWLEDGMENTS

We wish to thank Dr. W. K. Liu for his advice and assistance in this project. Support of the present research by a grant from the National Science Fouhdation is gratefully acknowledged. In addition, we wish to thank Control Data B. V., The Hague, for making available the computing facilities at the E. C. N.–N.S.P. Rekencentrum, Petten, North Holland, The Netherlands, where certain parts of these computations were performed. A portion of the work was performed while both authors were at the University of Illinois, and we are pleased to acknowledge support of this work there.

APPENDIX A: REMARKS ON SAMPLING

The cross sections were calculated using a random sampling[2] of the variables $\hat{j}_p$, $\hat{h}$, $\hat{j}$, $\hat{q}_{jp}$, $\hat{q}_l$, $\hat{q}_j$, and $\hat{q}_h$. Since p_R is known, one knows $\hat{l}$ when b has been selected ($\hat{l} = p_R b$). The impact parameter b was chosen by randomly sampling the variable $x_b = \exp(-b^2/\bar{b}^2)$ over the interval $[0, 1]$, where $\bar{b}$ is a parameter selected for each collision system so that the curve of $P(j, b)$ vs b generated in the Monte Carlo evaluation is reasonably well approximated by the plot of x_b vs b. Such a plot is shown for HCl–HCl, $j = 4$ in Fig. 5. The numerical values of $P(j, b)$ (the circles) are the averages over each interval of 1 a.u. on the b axis; the dashed curve represents the Gaussian function x_b. For HCl–HF and HCl–HCl, the values of the Gaussian parameters $\bar{b}$ are, respectively, 12 and 10 a.u. The choices of $\bar{b}$ are well justified by the 3% or less standard deviations in the average total inelastic cross sections in Table I. The variables $\hat{j}_p$, $\hat{h}$, and $\hat{J}$ are replaced by new variables[2(b)] x_{jp}, x_h, and x_J, defined as $\exp(-B_p \hat{j}_p^2/k_B T)$, $[\hat{h}^2 - (\hat{j}_p - \hat{l})^2]/4\hat{j}_p\hat{l}$, $[\hat{J}^2 - (\hat{h} - \hat{j})^2]/4\hat{h}\hat{j}$, each of which lie in (0, 1) and whose volume element $dx_{jp}\,dx_h\,dx_J$ equals the corresponding volume element in (6) (noting that the $1/Q_p$ in ρ_{jp} equals $B_p/k_B T$, where $T = 300\,^\circ$K). More details about the sampling and calculations were given earlier.[2(b)] Some 4000 trajectories were used for each j to obtain the distribution of j''s and hence to obtain each column of Tables II and III, while 2000 trajectories were used for each j in the case of Table V in Appendix B.

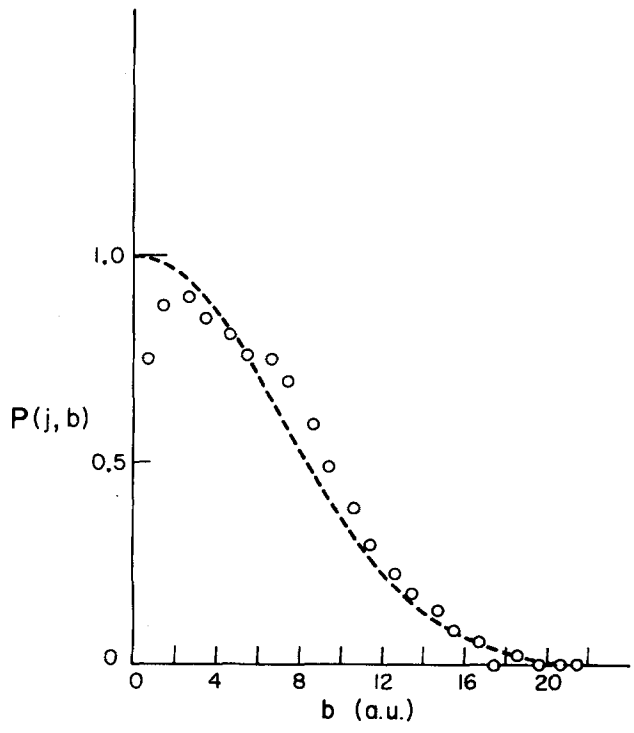

FIG. 5. Plot of $P(j, b)$ vs b for HCl–HCl, $j = 4$. The dashed curve is a plot of $x_b \equiv \exp(-b^2/\bar{b}^2)$ vs b, where $\bar{b} = 10$ a.u.

TABLE V. Rotational cross sections (Å^2) $\sigma(j,j')$ for HCl–HI and HCl–HBr.

j' \ j	0	4	8
		HCl–HI	
0		0.1±0.05	
1	40.8±2.5	0.7±0.1	
2	13.4±0.7	4.0±0.4	
3	5.6±0.4	18.4±1.3	
4	0.8±0.2		
5		19.6±1.7	0.06±0.03
6		2.7±0.3	2.0±0.3
7		0.07±0.04	10.7±1.0
8			
9			6.7±0.5
10			0.3±0.1
11			
		HCl–HBr	
0		0.8±0.2	
1	48.7±3.9	3.9±0.4	
2	21.0±1.1	9.5±0.7	
3	11.1±0.7	30.2±2.1	0.2±0.1
4	7.5±0.5		1.3±0.2
5	2.5±0.3	28.1±2.5	3.6±0.4
6	0.2±0.1	7.0±0.6	6.5±0.6
7		2.1±0.3	18.0±1.5
8		0.7±0.2	
9		0.04±0.04	11.7±0.8
10			2.9±0.4
11			0.2±0.1
12			

APPENDIX B: CALCULATIONS FOR HCl–HI AND HCl–HBr SYSTEMS

For HI the values used for ϵ/k, σ, μ, B, α'', and $\alpha^{\perp}$ were 289 °K,[5] 4.211 Å,[5] 0.44 D,[6] 6.551 cm^{-1},[7] 6.58 Å^3,[9] and 4.89 Å^3,[9] respectively. The corresponding values used for HBr were 449, 3.353, 0.82, 8.473, 4.22, and 3.31 (same references). The values of $\sigma(j,j')$ calculated from the present potential are given in Table V for the HCl–HI and HCl–HBr systems. One also finds that the $\sigma(j)$'s for HCl–HI collisions are 20±1, 46±2, and 44±2 Å^2 for $j=8$, 4, 0, respectively, while those for HCl–HBr collisions are 44±2, 82±3, and 91±4 Å^2, respectively. From the results in Table V, one finds that C for HCl–HI is 0.016 cm, compared with a value inferred from experiment[3(a)] of 0.003, and C for HCl–HBr is 0.008 cm, compared with an experimental value[3(a)] of 0.004.

[1]For comprehensive review articles on trajectories, see (a) D. L. Bunker, Methods Comput. Phys. 10, 287 (1971); (b) R. N. Porter, Ann. Rev. Phys. Chem. 25, 317 (1974).

[2](a) A. F. Turfa, D. E. Fitz, and R. A. Marcus, J. Chem. Phys. 67, 4463 (1977); (b) A. F. Turfa, W. K. Liu, and R. A. Marcus, J. Chem. Phys. 67, 4468 (1977).

[3](a) A. M. G. Ding and J. C. Polanyi, Chem. Phys. 10, 39 (1975); (b) J. C. Polanyi and K. B. Woodall, J. Chem. Phys. 56, 1563 (1972); (c) J. C. Polanyi, N. Sathyamurthy, and J. L. Schreiber, J. Chem. Phys. 24, 105 (1977); (d) N. C. Lang, J. C. Polanyi, and J. Wanner, *ibid.* 24, 219 (1977); (e) J. C. Polanyi and N. Sathyamurthy, *ibid.* 29, 9 (1978).

[4]W. H. Wong, University of Toronto, unpublished work [Ref. 22 in Ref. 3(a)].

[5]R. C. Reid and T. K. Sherwood, *The Properties of Gases and Liquids* (McGraw-Hill, New York, 1966), 2nd ed.

[6]R. D. Nelson, Jr., D. R. Lide, Jr., and A. A. Maryott, *Selected Values of Electric Dipole Moments for Molecules in the Gas Phase*, Natl. Stand. Ref. Data Ser. Natl. Bur. Stand. 10 (1967).

[7]G. Herzberg, *Spectra of Diatomic Molecules* (Van Nostrand, New York, 1950), 2nd ed.

[8]N. J. Bridge and A. D. Buckingham, Proc. R. Soc. London Ser. A 295, 334 (1966).

[9]Landolt–Börnstein, *Zahlenwerte und Funktionen*, Band I, Teil 3 (Springer, Berlin, 1950), p. 510.

[10]J. M. Hammersley and D. C. Handscomb, *Monte Carlo Methods* (Wiley, New York, 1964).